

Electronic Supporting Information for

Substituted Stilbene-based Oxime Esters used as Highly Reactive Wavelength-dependent Photoinitiators for LEDs Photopolymerization

Shixiong Chen^a, Ming Jin^{*.a}, Jean-Pierre Malval^{*.b}, Jingming Fu^a, Fabrice Morlet-Savary^b, Haiyan Pan^a, Decheng Wan^a

^aDepartment of Polymer Materials, School of Materials Science and Engineering, Tongji University, 4800 Caoan Road, Shanghai, 201804, P.R. China

^bInstitut de Science des Matériaux de Mulhouse, UMR CNRS 7361, Université de Haute-Alsace, 15 rue Jean Starcky, Mulhouse, 68057, France

Correspondence to: M. Jin (mingjin@tongji.edu.cn), J.P. Malval (jean-pierre.malval@uha.fr)

Table of Contents

Fig. S1	The experimental spectra and theoretical spectra of (a) MMM , (b) MME , (c) MMP , (d) MPE and (e) CPE in ACN
Fig. S2	The normalized UV-Vis spectrum of (a) MME , (b) MPE , (c) CME and (d) CPE in different solvents
Fig. S3	Evolution of the absorption spectra of (a) MMM , (b) MME , (c) MMP , (d) MPE and (e) CPE in ACN
Fig. S4	ESR-ST spectra obtained after light irradiation of CME and CPE in benzene (DMPO is used as spin-trap reactant).
Fig. S5	The DSC curve of OXEs in air (1 wt% in TMPTA, 10 K min ⁻¹)
Fig. S6	The GPC elution curve using CME or MME as the photoinitiators.
Table S1	The maximum absorption wavelength (λ_{\max}) of four OXEs in different solvents
Table S2	The change of integral area of the hydrogens
Table S3	GPC data results using CME or MME (0.1 wt%) as photoinitiator
Fig. S7-40	¹ H NMR, ¹³ C NMR and MS spectra of PIs and intermediate

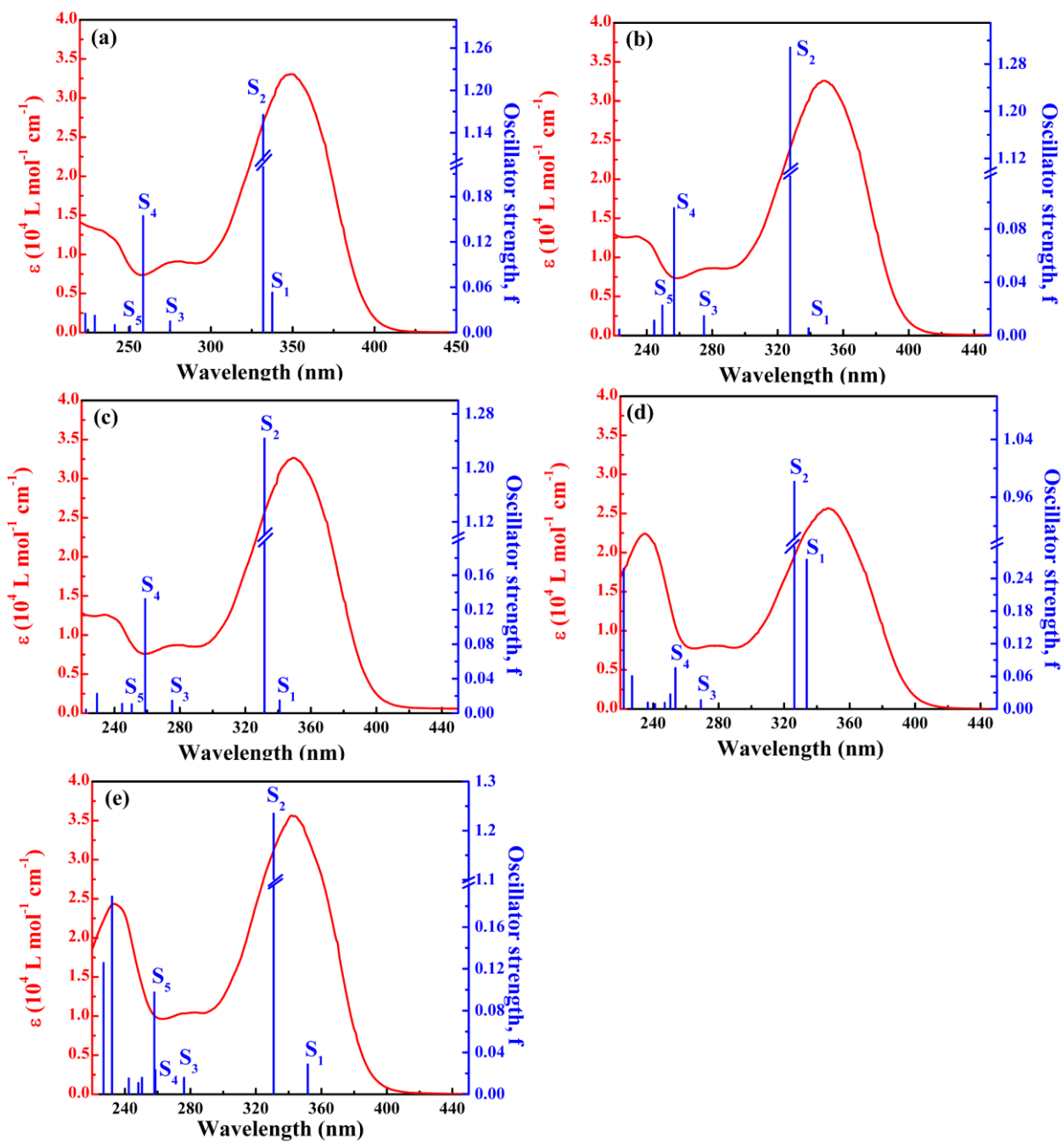


Fig. S1 The experimental spectra and theoretical spectra of (a) **MMM**, (b) **MME**, (c) **MMP**, (d) **MPE** and (e) **CPE** in ACN

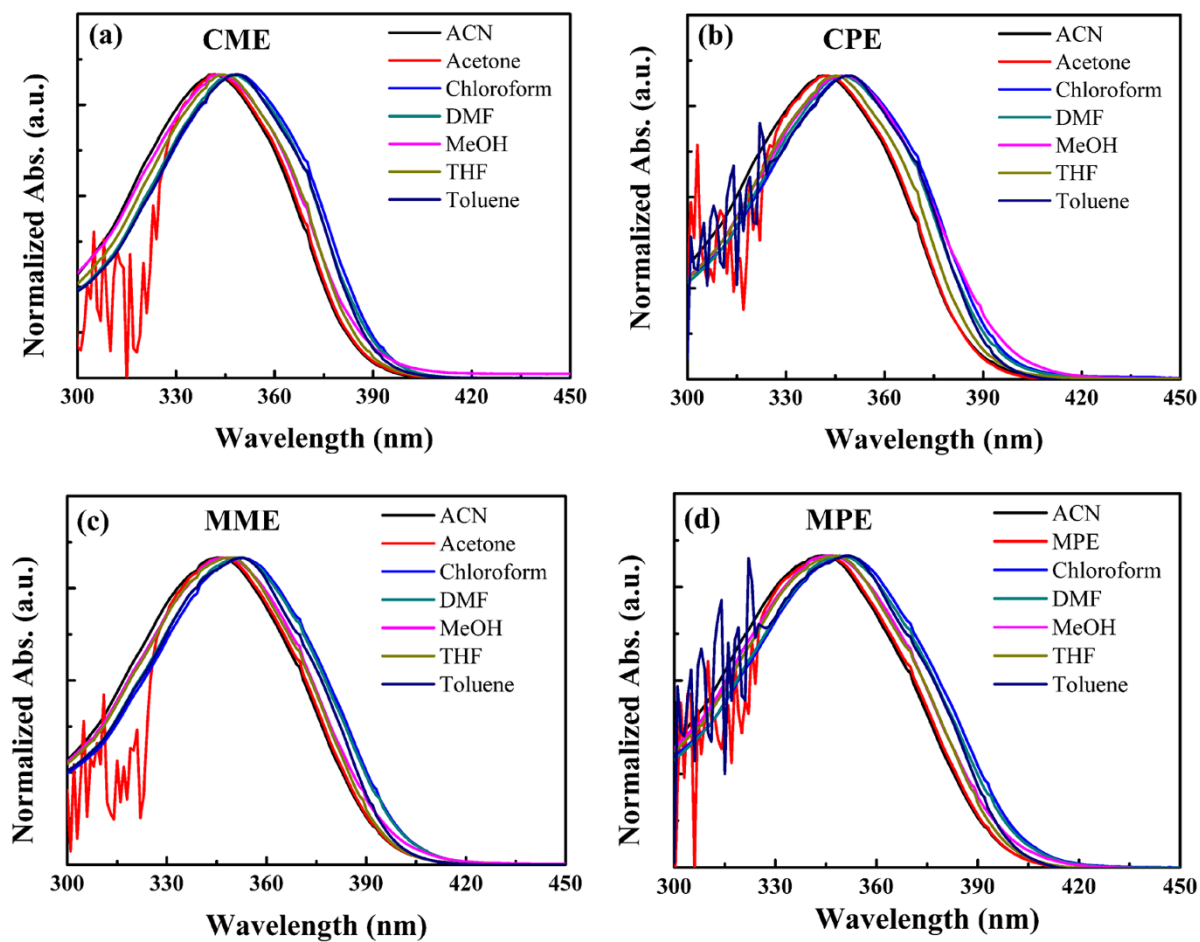


Fig. S2 The normalized UV-Vis spectrum of (a) MME, (b) MPE, (c) CME and (d) CPE in different solvents

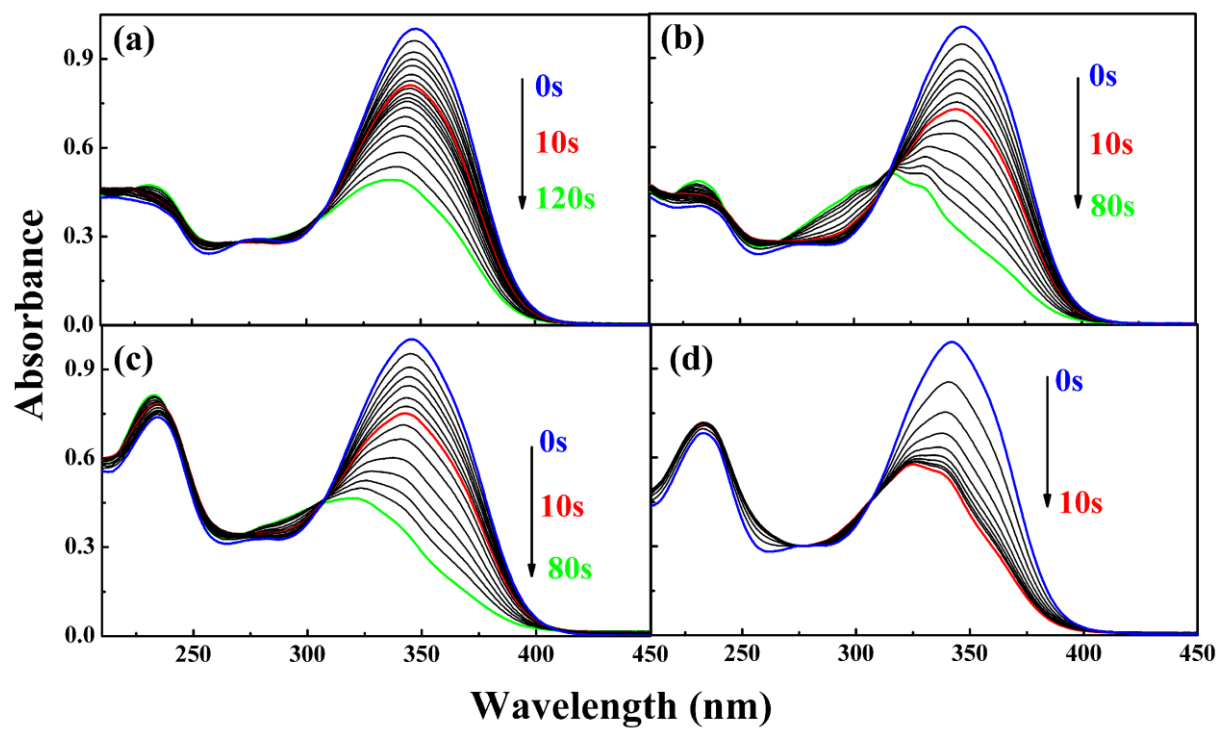


Fig. S3 Evolution of the absorption spectra of (a) **MMM**, (b) **MMP**, (c) **MPE** and (d) **CPE** in CAN

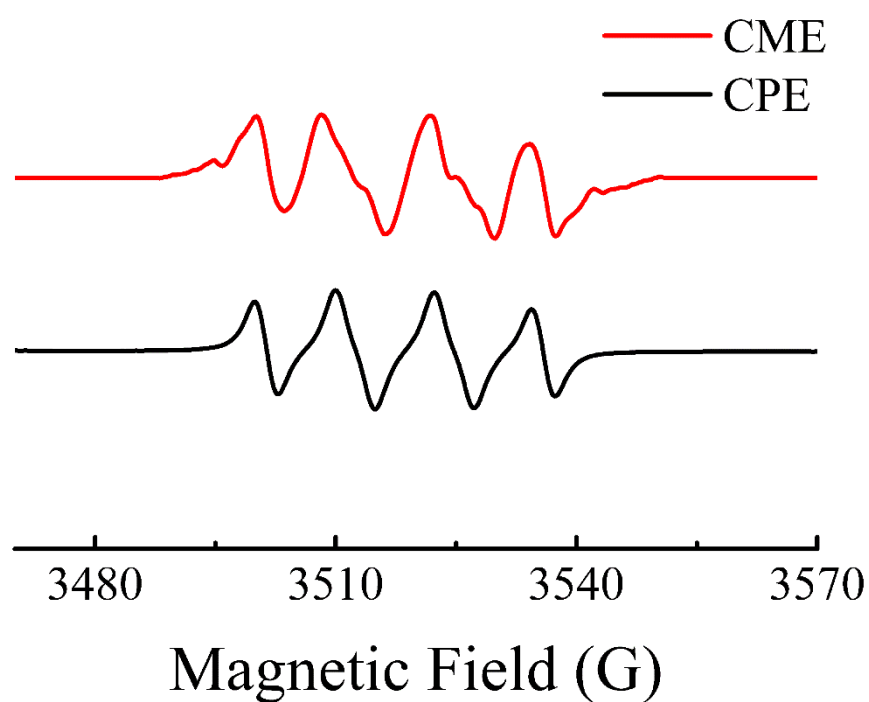


Fig. S4 ESR-ST spectra obtained after light irradiation of CME and CPE in benzene (DMPO is used as spin-trap reactant). For CME, $a_N = 14.50$ G, $a_H = 21.51$ G; for CPE, $a_N = 14.86$ G, $a_H = 22.29$ G).

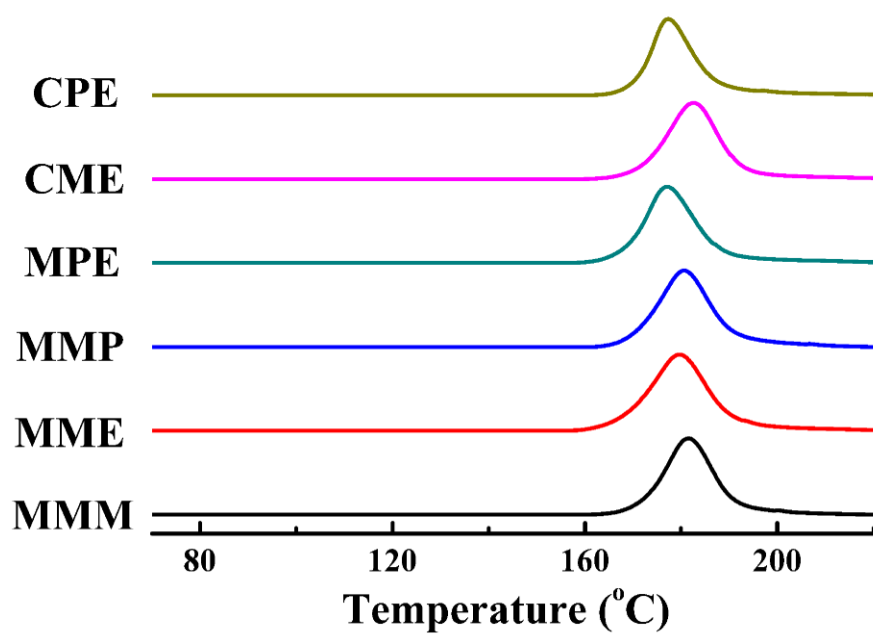


Fig. S5 The DSC curve of OXEs in air (1 wt% in TMPTA, 10 K min⁻¹)

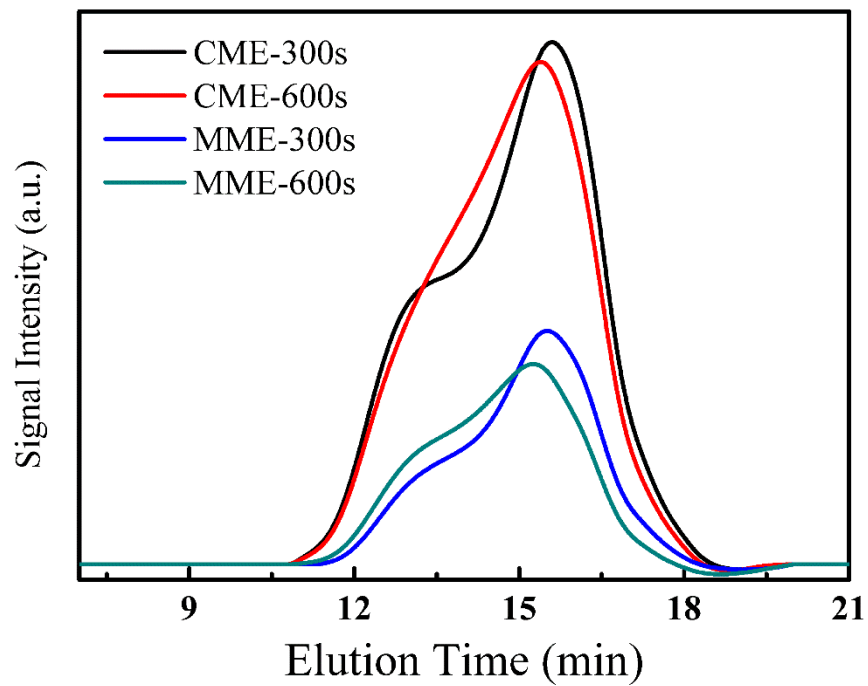


Fig. S6 The GPC elution curve using CME or MME as the photoinitiators.

OXEs	λ_{\max} (nm)						
	ACN	Acetone	Chloroform	DMF	MeOH	THF	Toluene
CME	342	341	349	347	343	344	348
CPE	341	342	349	347	343	345	350
MME	348	347	353	352	349	348	348
MPE	344	345	351	349	347	348	352

Table S1 The maximum absorption wavelength (λ_{\max}) of four OXEs in different solvents

	Relative changes of the integrated ¹ H-NMR signal								
	1	1'	2	2'	3	3'	3''	4	4'
0min	0	0	0	0	0	0	0	0	0
5min	-0.32	0.23	-0.13	0.12	-0.7	0.46	0.04	-0.73	0.47
10min	-0.88	0.62	-0.34	0.31	-0.98	0.68	0.16	-1.44	0.84
20min	-1.39	0.84	-0.63	0.43	-1.48	0.92	0.32	-2.19	1.32
30min	-1.63	0.78	-0.71	0.45	-1.76	0.98	0.57	-2.64	1.23

Table S2. The change of integral area of the hydrogens (ΔI , $\Delta I = I_t - I_0$. It is the integral area when irradiated for t minutes. I_0 is the initial integral area of the origin peaks) at different time under irradiation at 365 nm LED (The integral area of peaks is calculated when the integral of all the aryl peaks are 10.)

OXE	Irradiation Time	$M_n (\times 10^5 \text{ g mol}^{-1})$	$M_w (\times 10^5 \text{ g mol}^{-1})$	M_w/M_n	Conversion (%)
CME	300s	1.47	5.99	4.07	20.59
	600s	1.65	5.94	3.60	33.33
MME	300s	1.28	4.01	3.13	11.80
	600s	1.84	5.78	3.14	22.59

Table S3 GPC data results using CME or MME (0.1 wt%) as photoinitiator

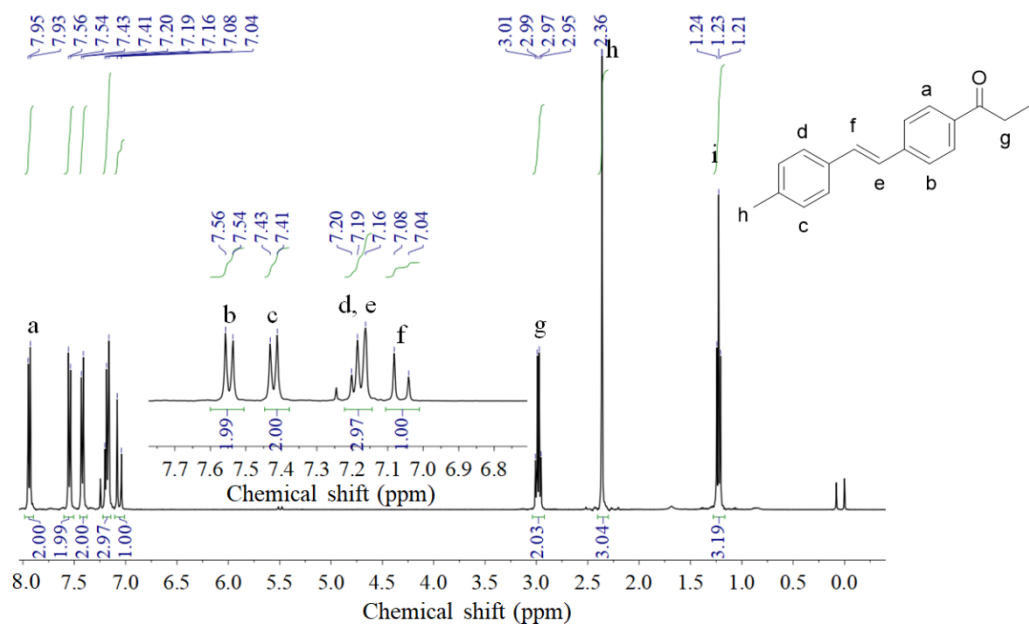


Fig. S7 ¹H-NMR spectra of **1a** in CDCl₃

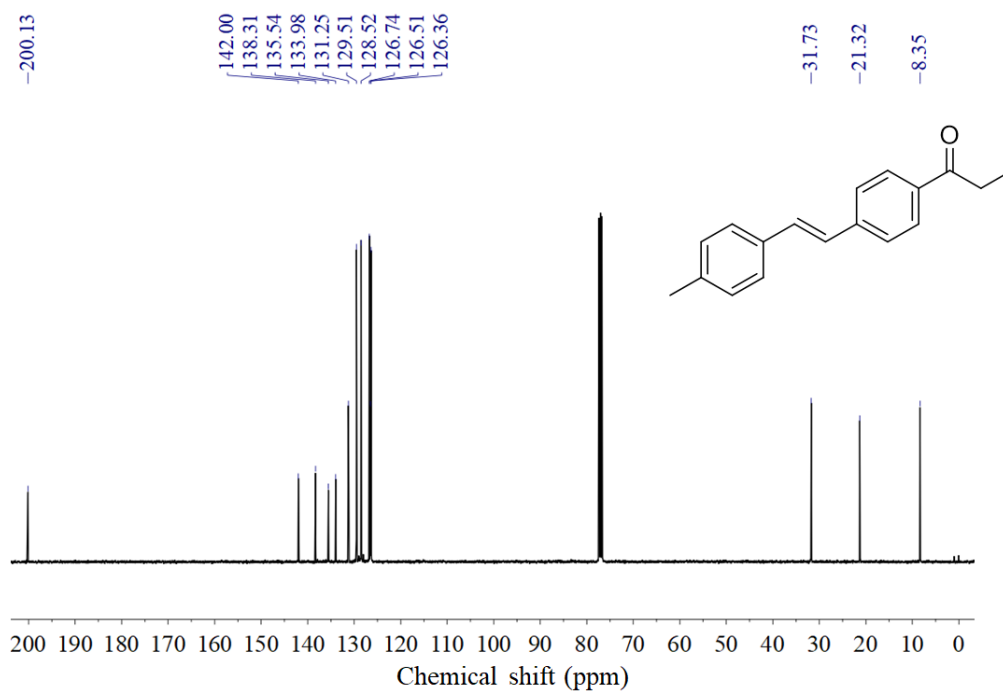


Fig. S8 ¹³C-NMR spectrum of **1a** in CDCl₃

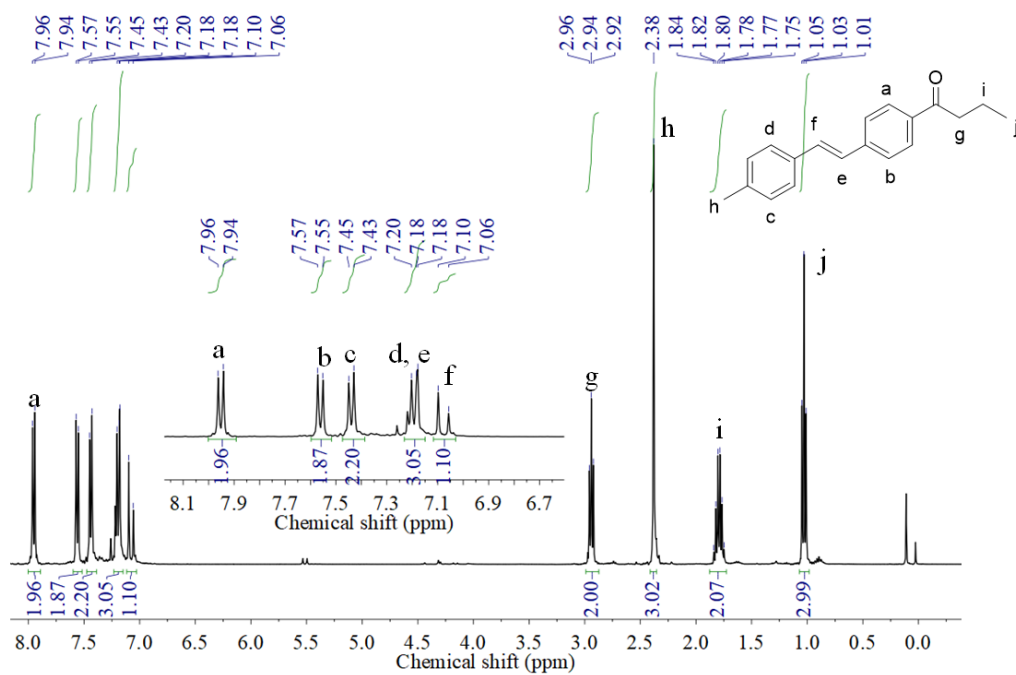


Fig. S9 ¹H-NMR spectrum of **1b** in CDCl₃

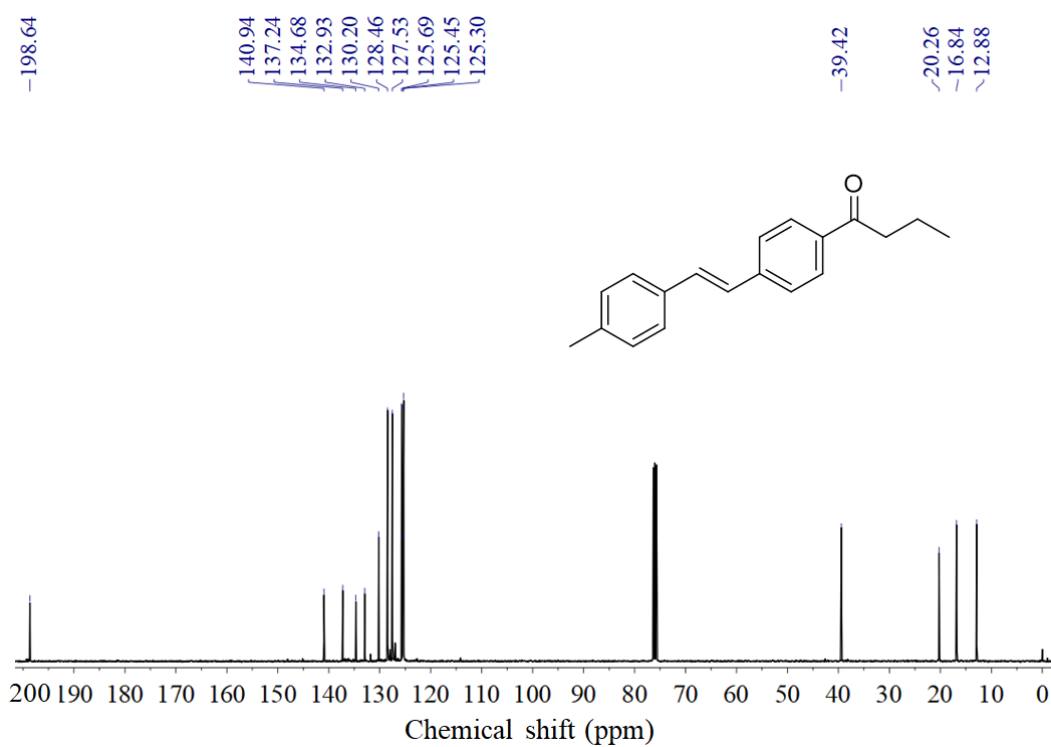


Fig. S10 ¹³C-NMR spectrum of **1b** in CDCl₃

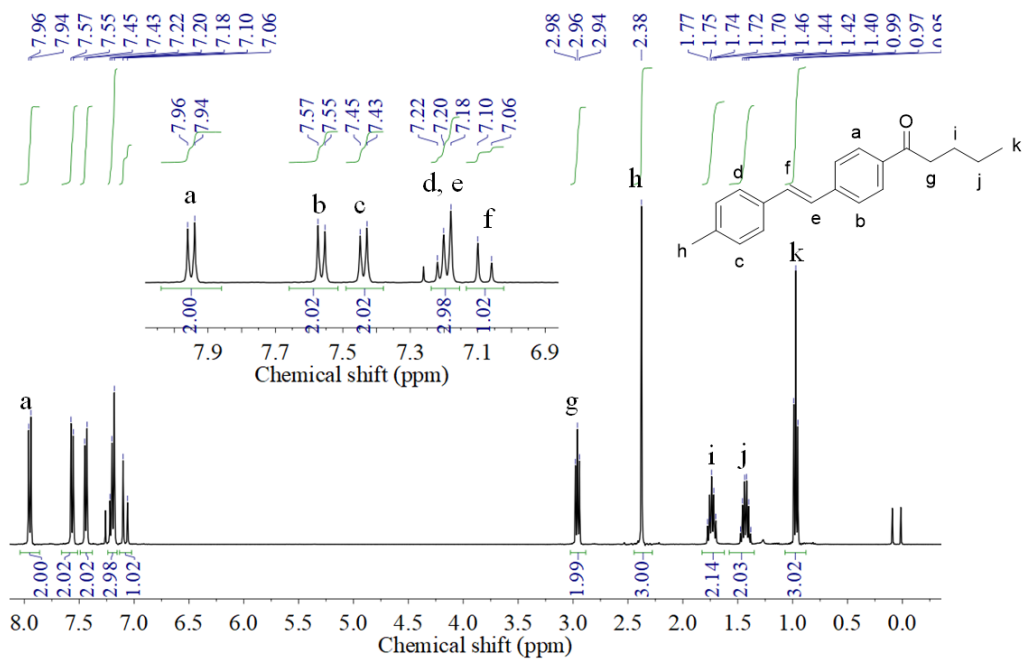


Fig. S11 ¹H-NMR spectrum of **1c** in CDCl₃

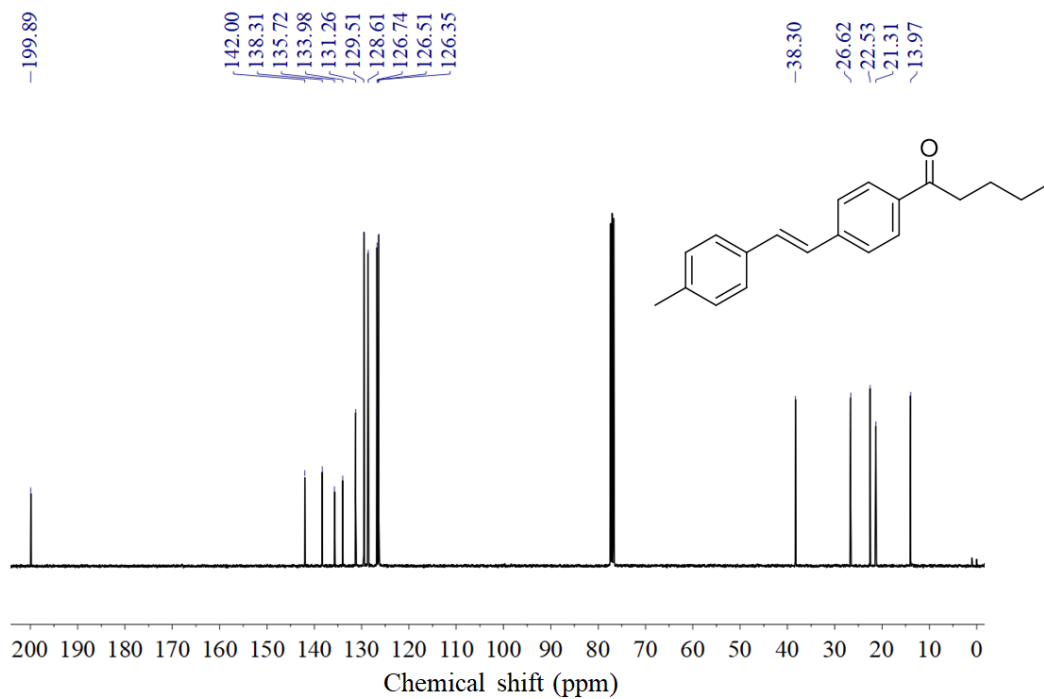


Fig. S12 ¹³C-NMR spectrum of **1c** in CDCl₃

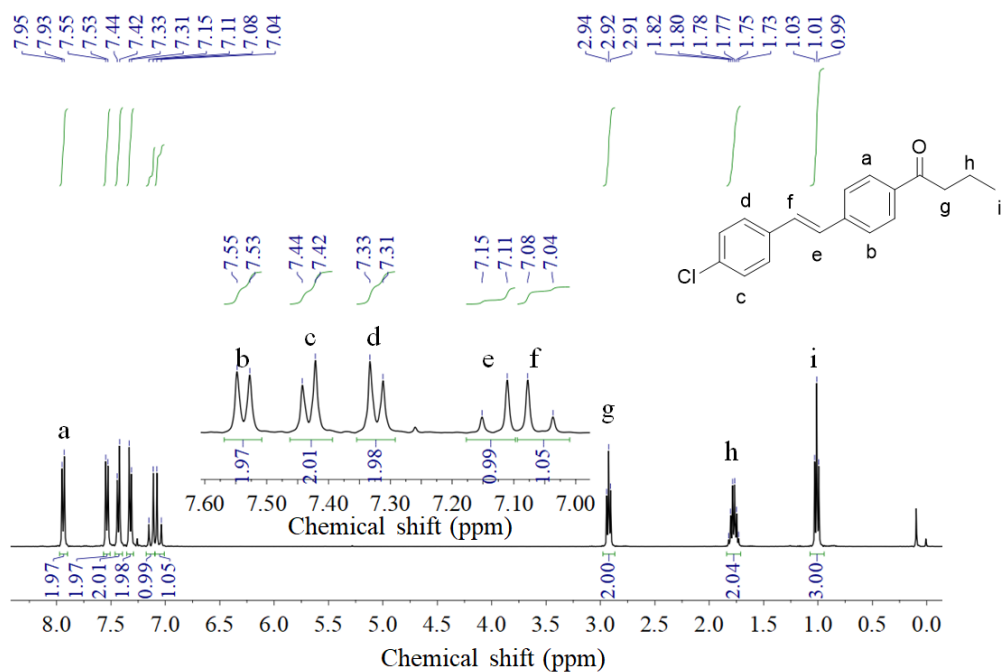


Fig. S13 ¹H-NMR spectrum of **1d** in CDCl₃

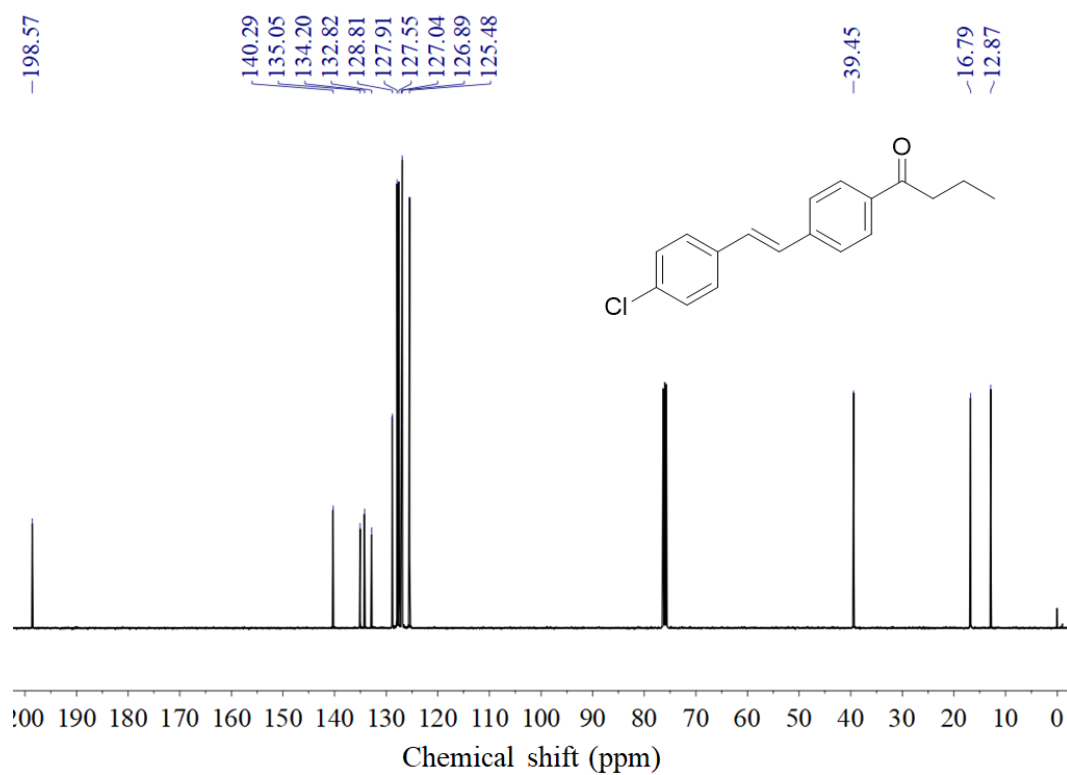


Fig. S14 ¹³C-NMR spectrum of **1d** in CDCl₃

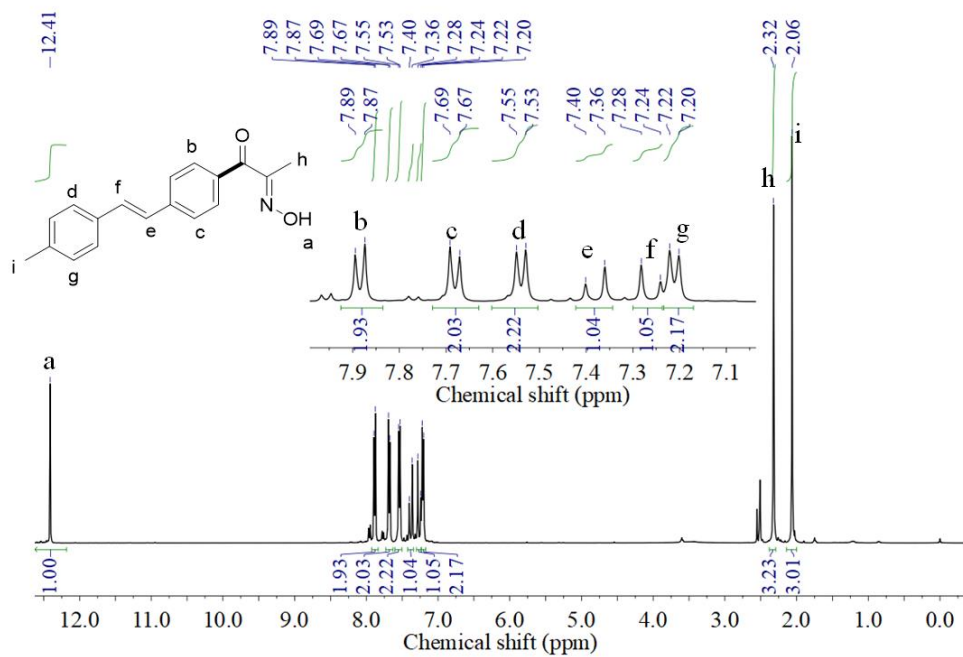


Fig. S15 $^1\text{H-NMR}$ spectrum of **2a** in $\text{DMSO-}d_6$

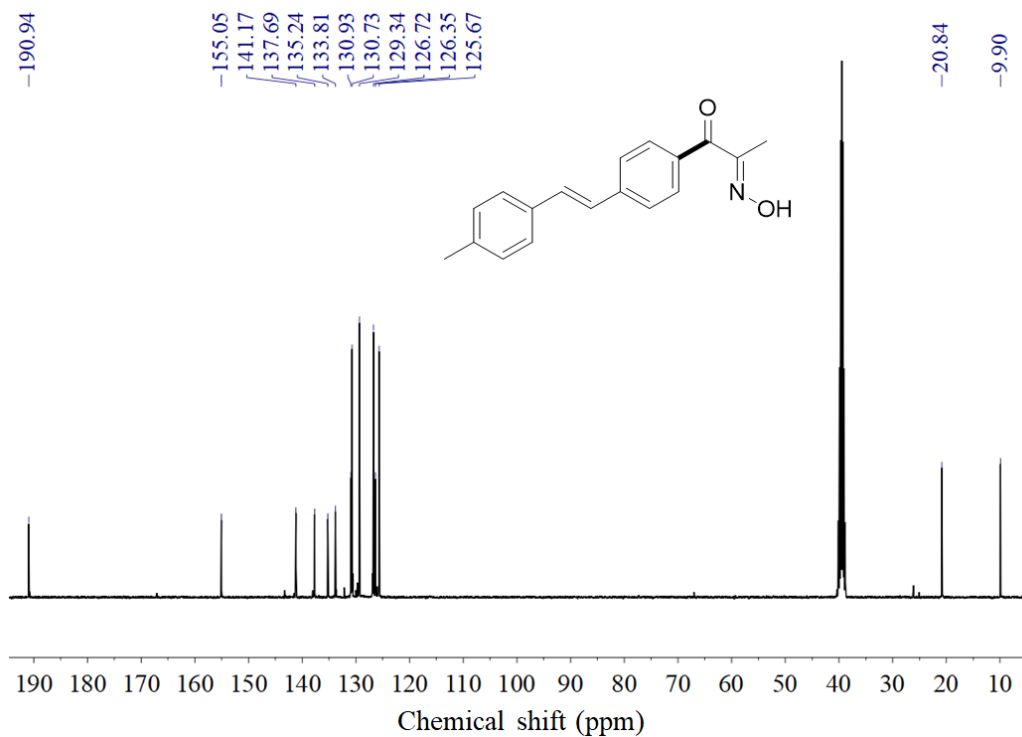


Fig. S16 $^{13}\text{C-NMR}$ spectra of **2a** in $\text{DMSO-}d_6$

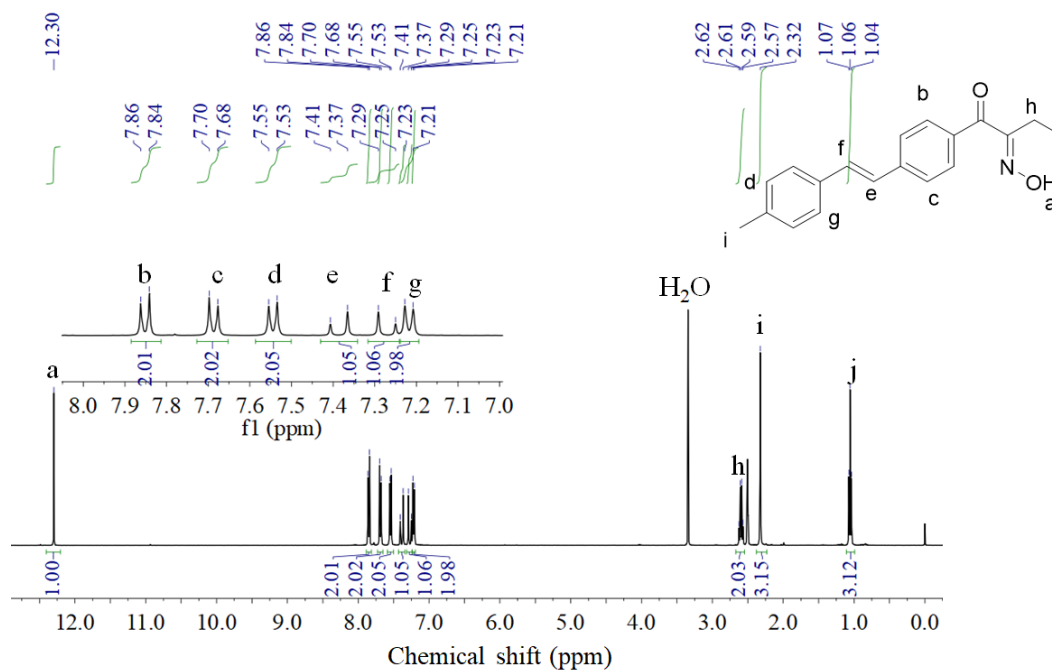


Fig. S17 $^1\text{H-NMR}$ spectrum of **2b** in $\text{DMSO-}d_6$

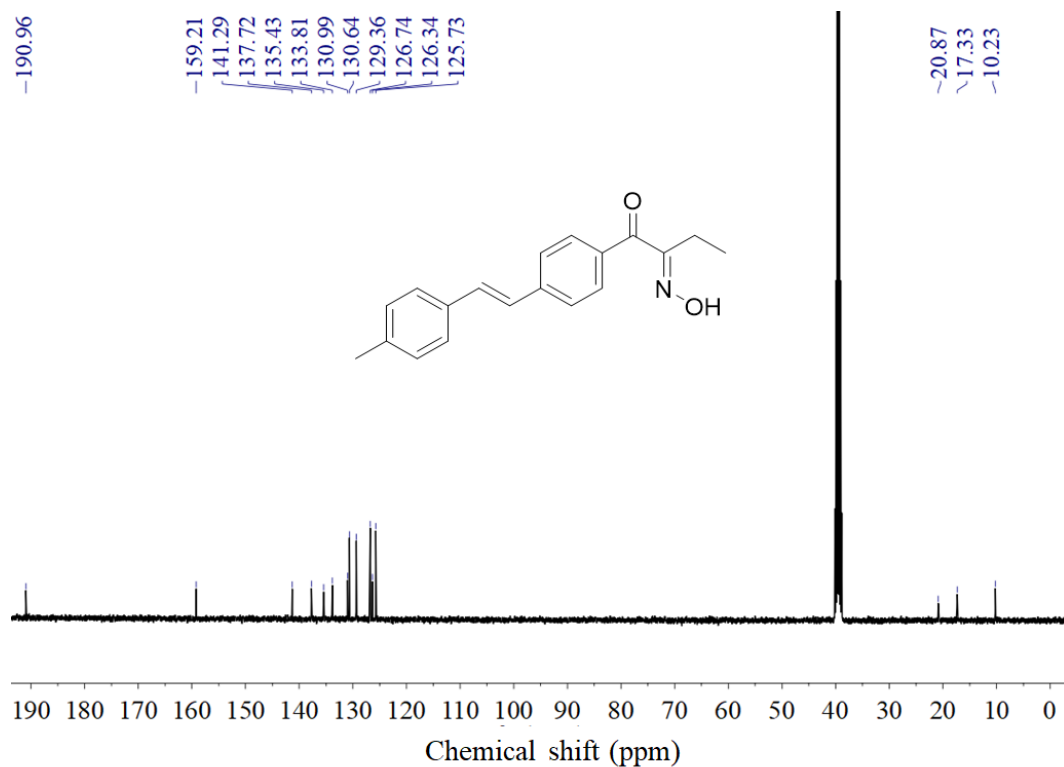


Fig. S18 $^{13}\text{C-NMR}$ spectrum of **2b** in $\text{DMSO-}d_6$

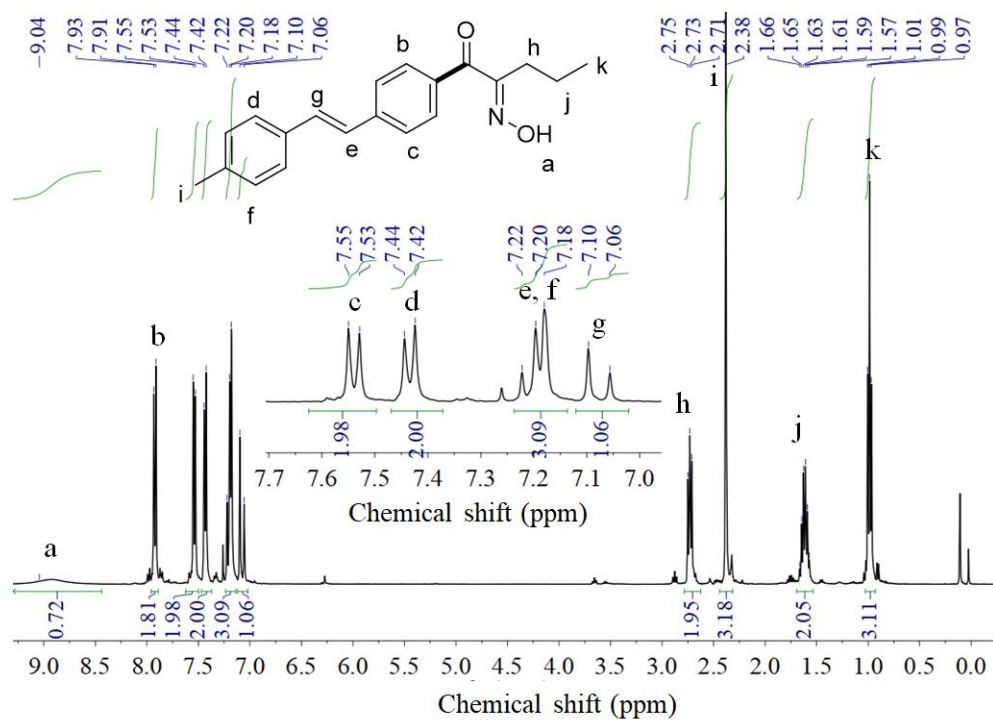


Fig. S19 $^1\text{H-NMR}$ spectrum of **2c** in CDCl_3

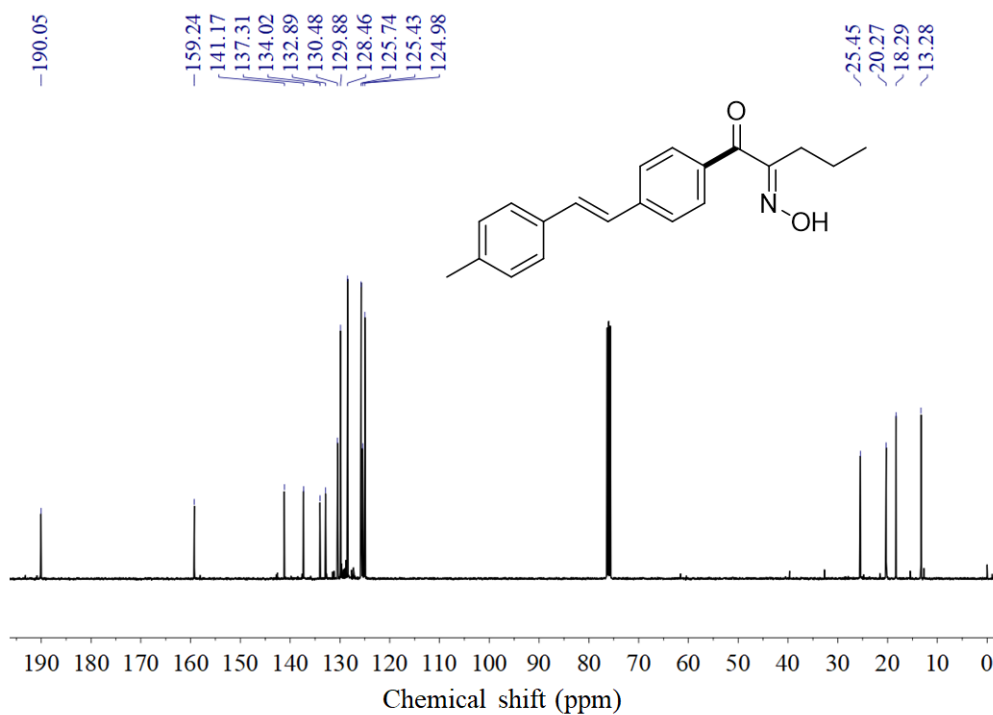


Fig. S20 $^{13}\text{C-NMR}$ spectrum of **2c** in CDCl_3

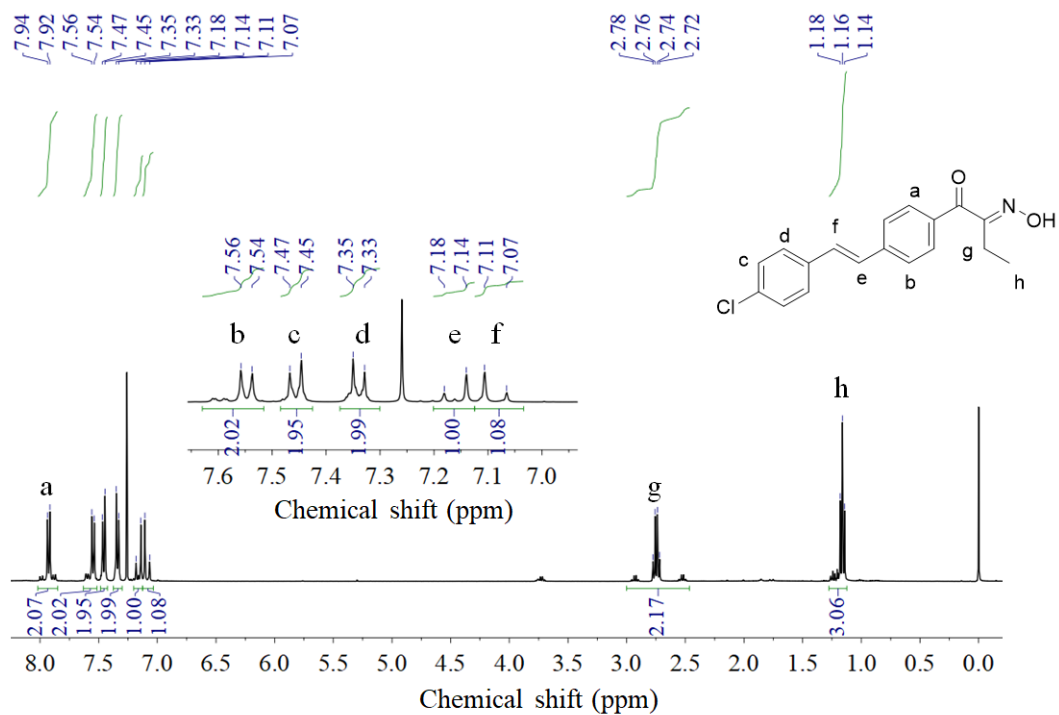


Fig. S21 $^1\text{H-NMR}$ spectrum of **2d** in CDCl_3

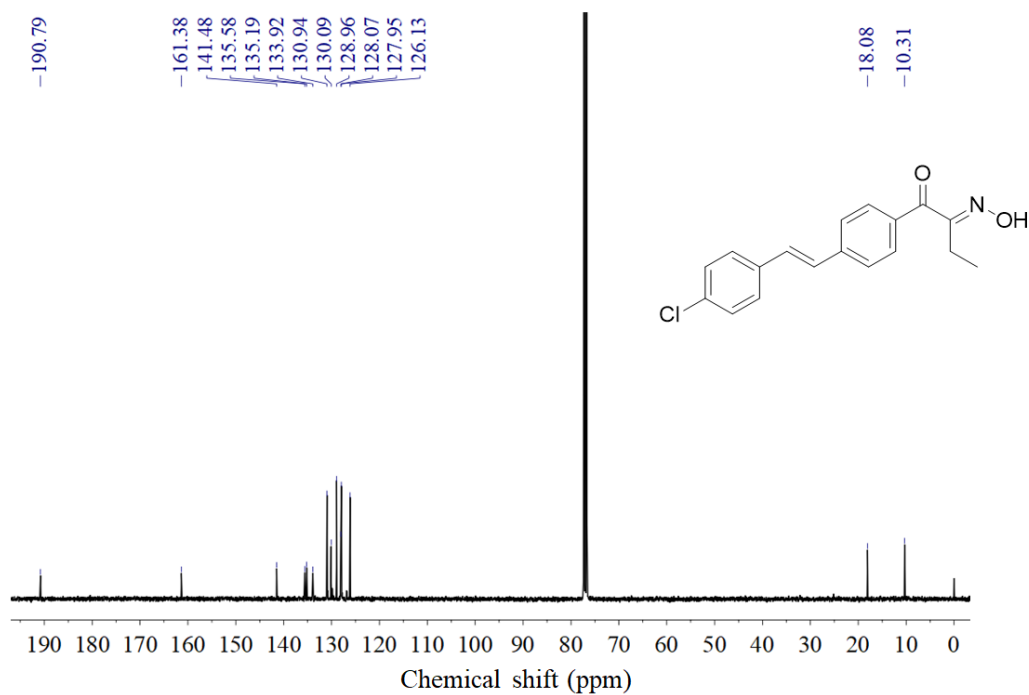


Fig. S22 $^{13}\text{C-NMR}$ spectrum of **2d** in CDCl_3

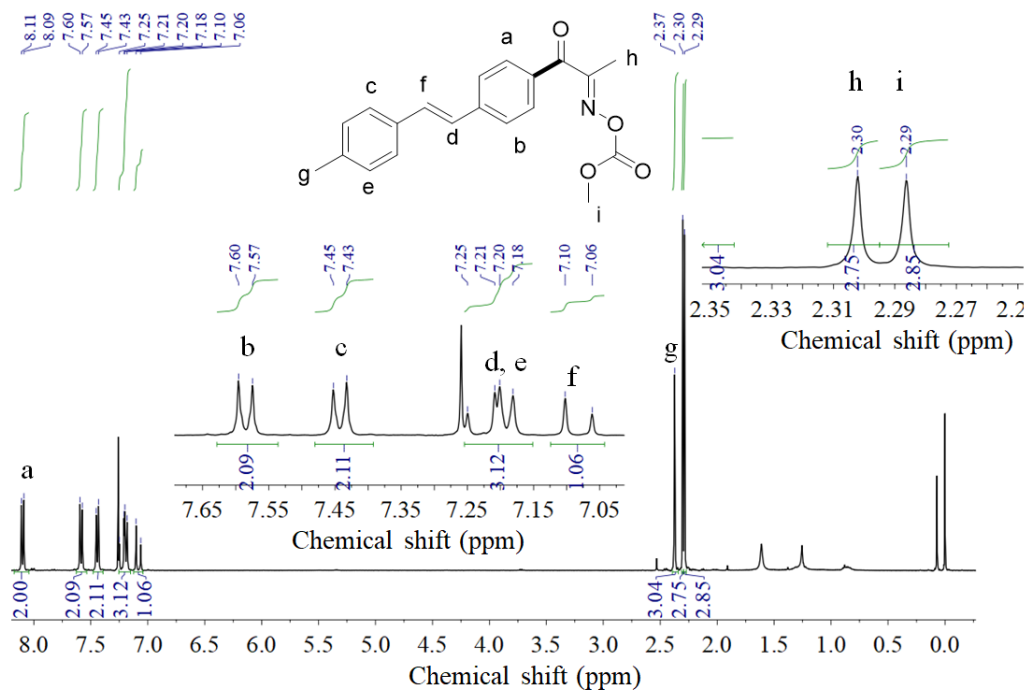


Fig. S23 $^1\text{H-NMR}$ spectrum of **MMM** in CDCl_3

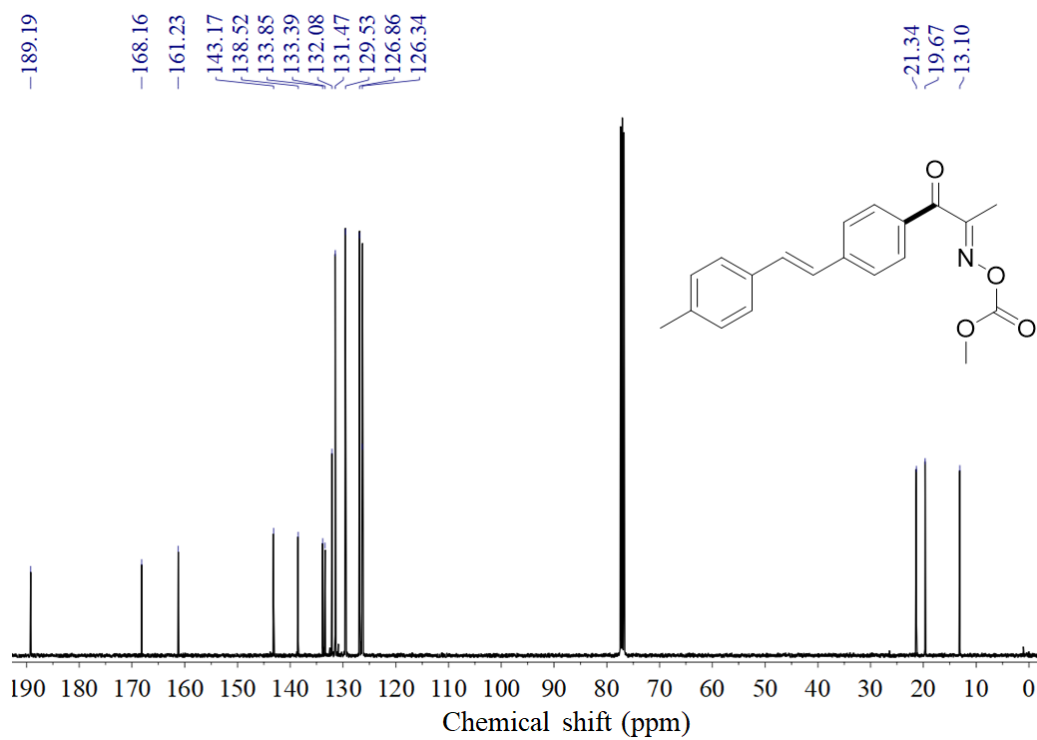


Fig. S24 $^{13}\text{C-NMR}$ spectrum of **MMM** in CDCl_3

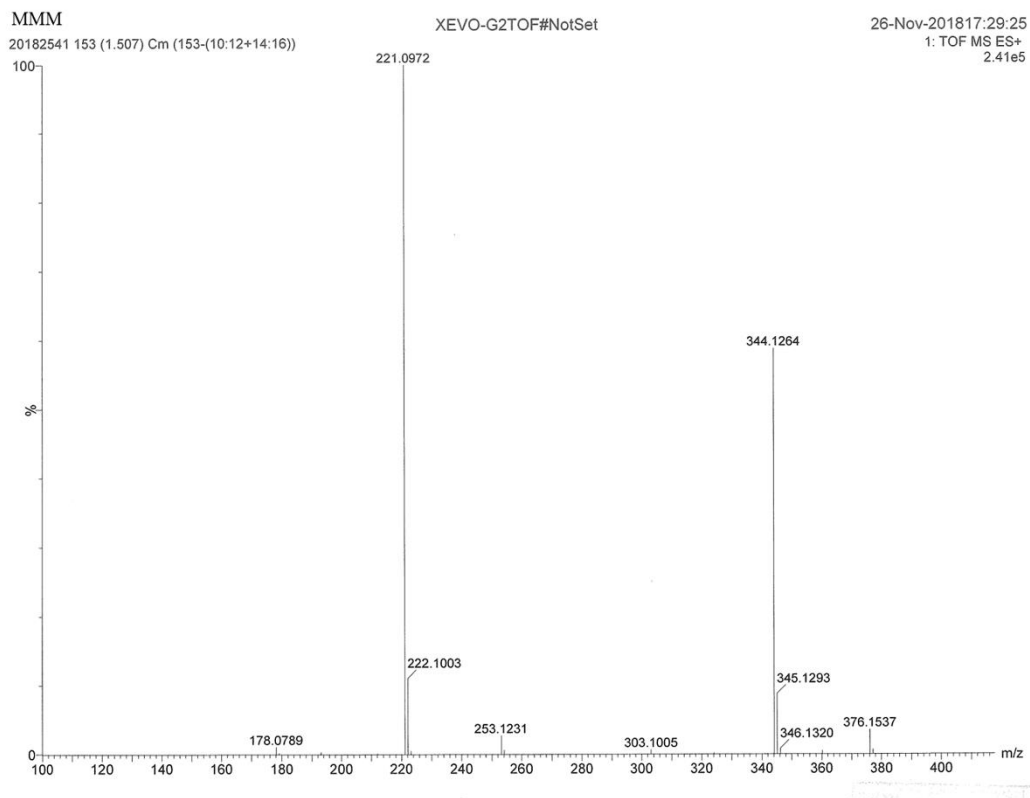


Fig. S25 MS of MMM

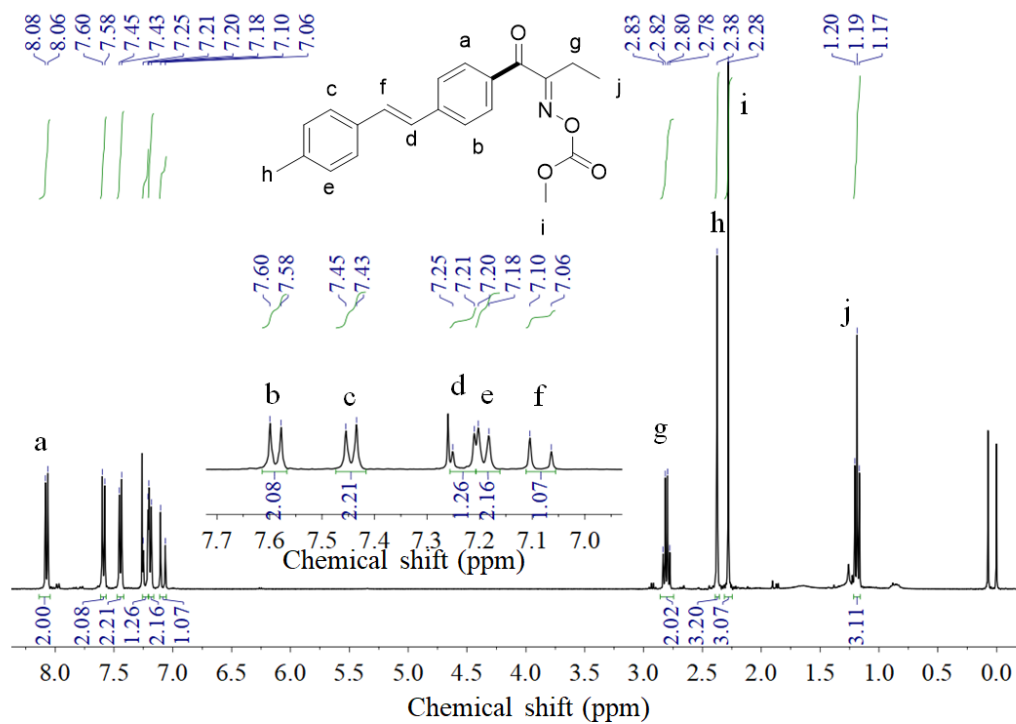


Fig. S26 $^1\text{H-NMR}$ spectrum of MME in CDCl_3

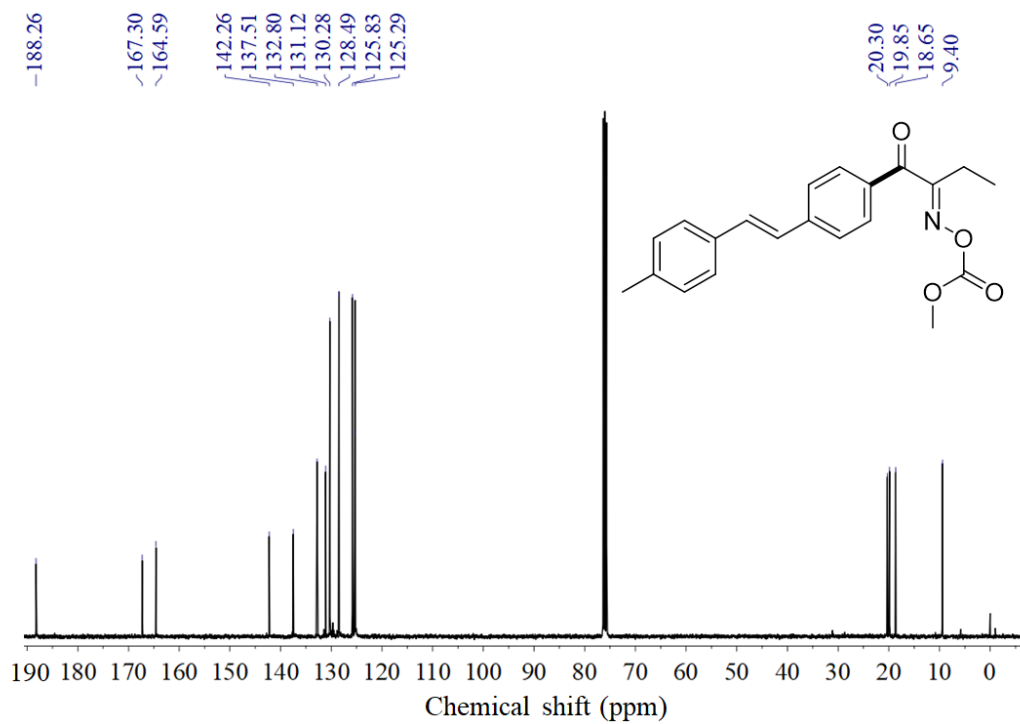


Fig. S27 ¹³C-NMR spectrum of MME in CDCl₃

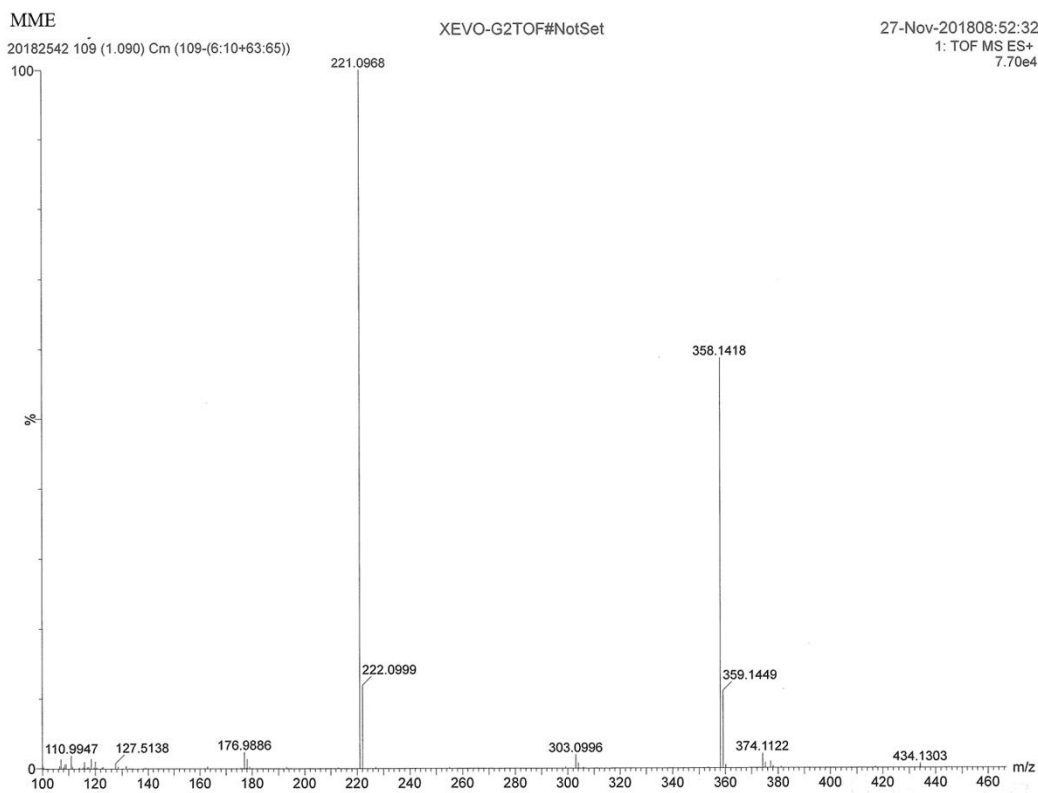


Fig. S28 MS of MME

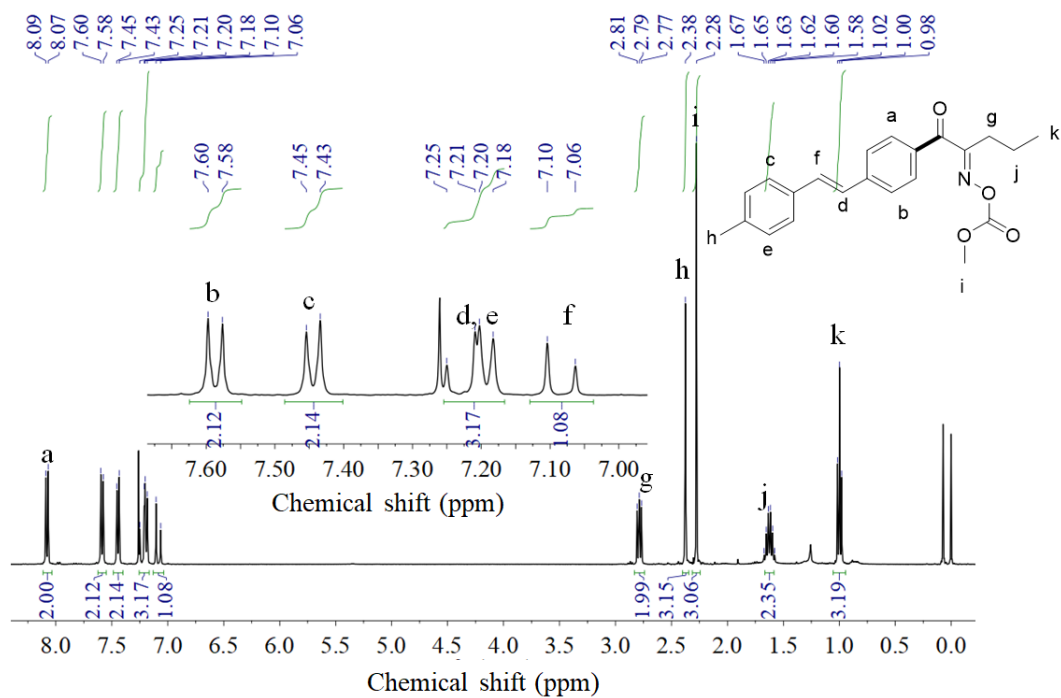


Fig. S29 ^1H -NMR spectrum of **MMP** in CDCl_3

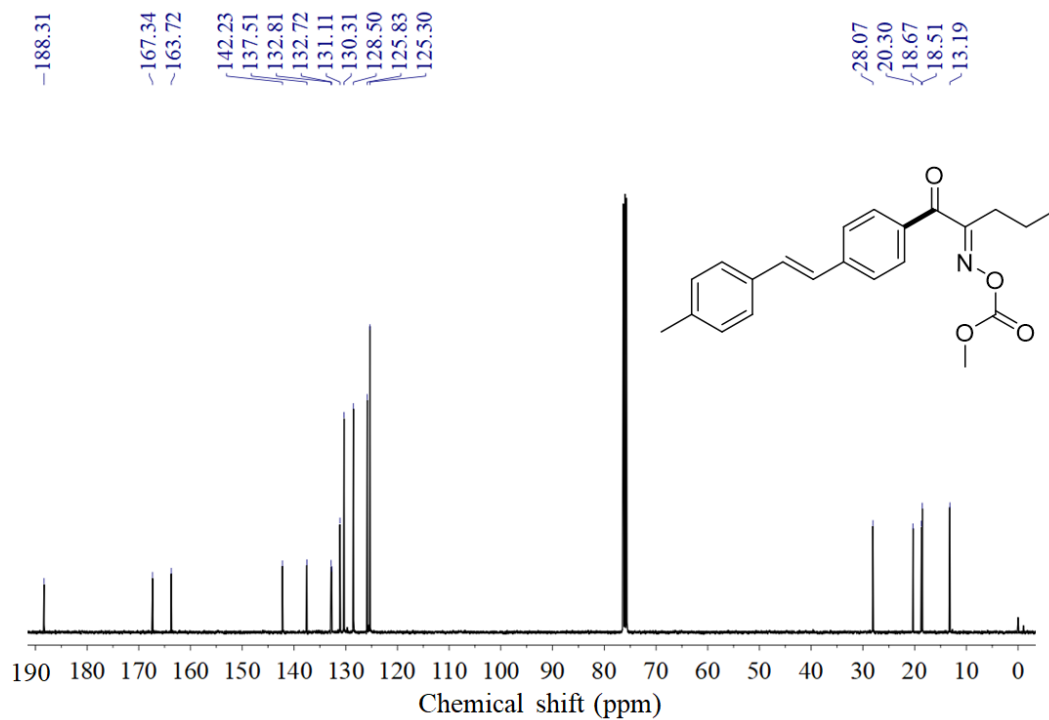


Fig. S30 ^{13}C -NMR spectrum of **MMP** in CDCl_3

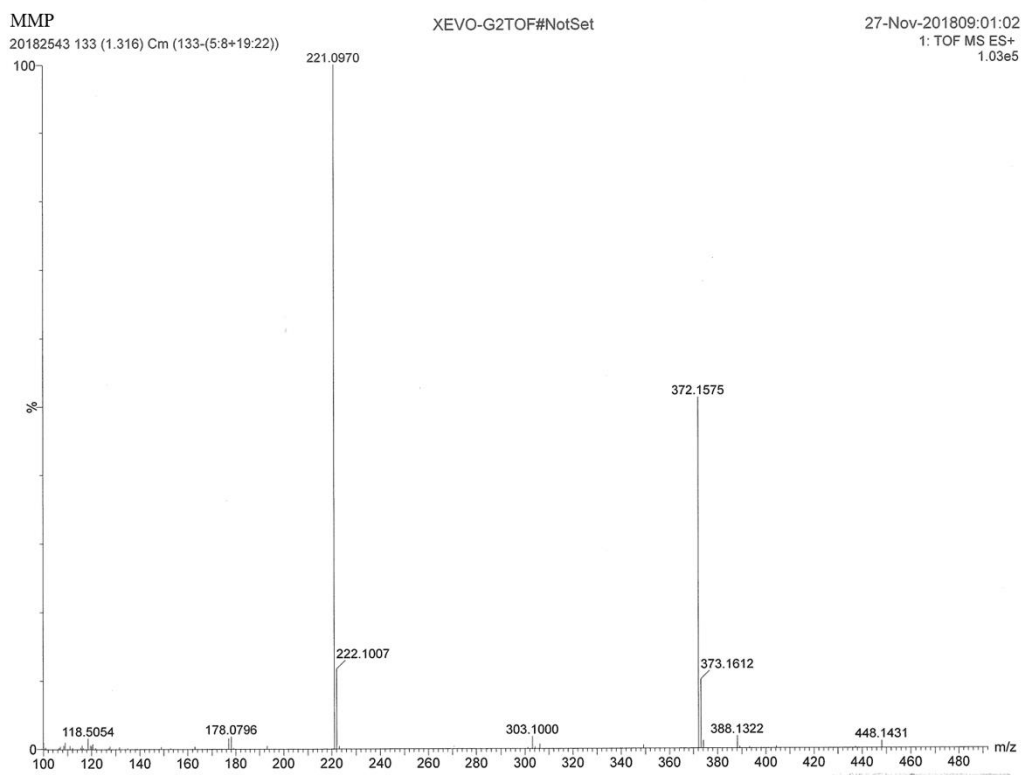


Fig. S31 MS of MMP

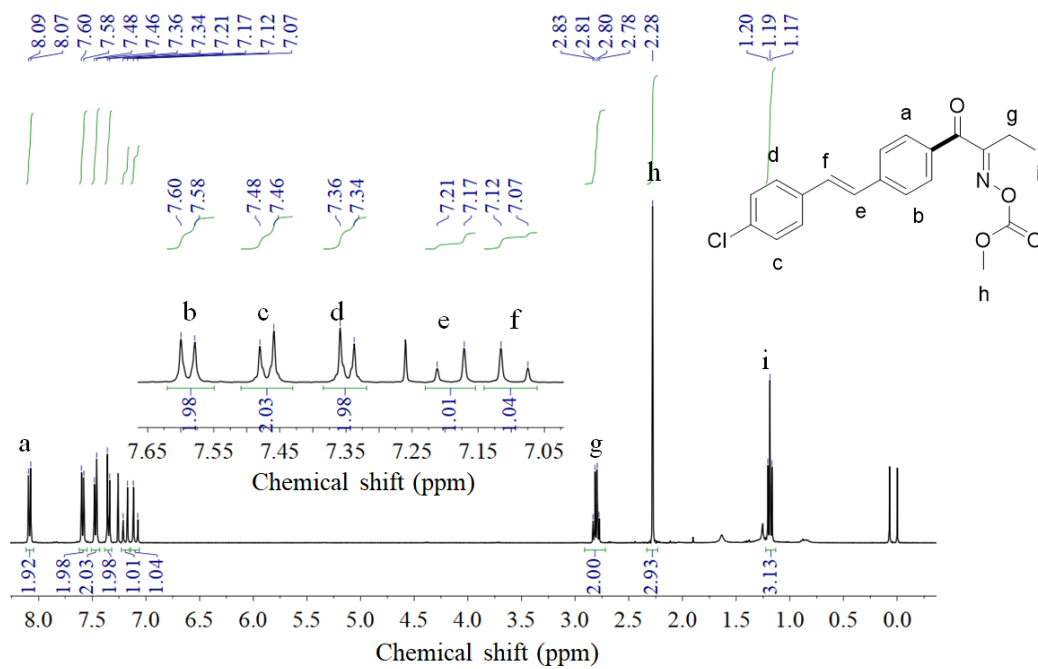


Fig. S32 ¹H-NMR spectrum of CME in CDCl₃

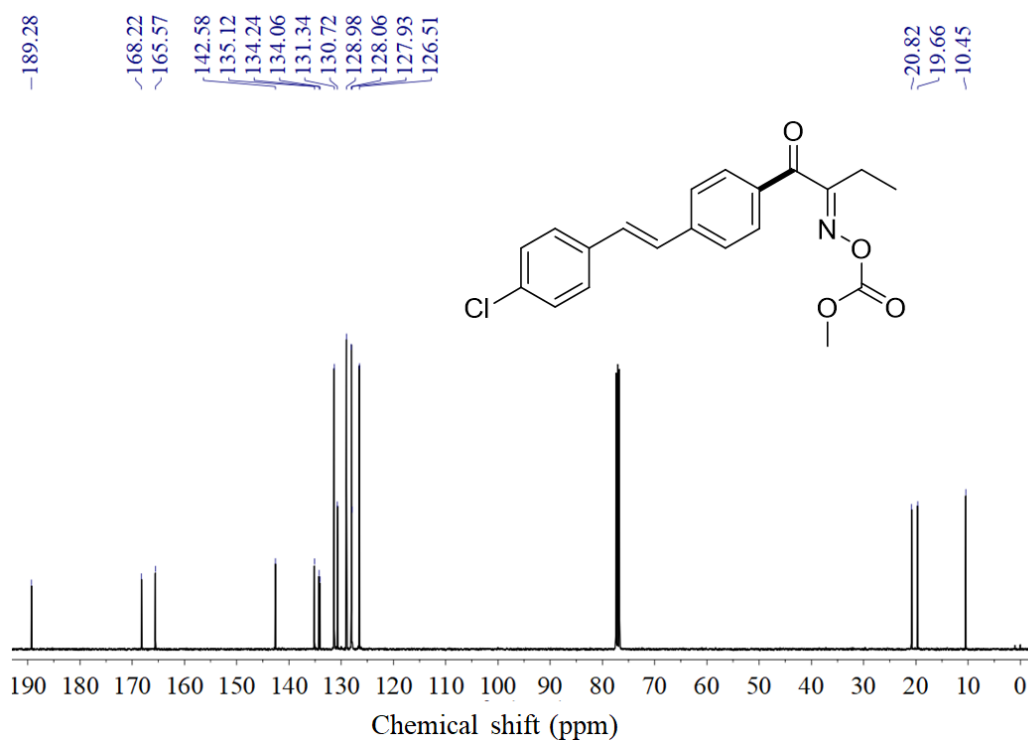


Fig. S33 ¹³C-NMR spectrum of CME in CDCl₃

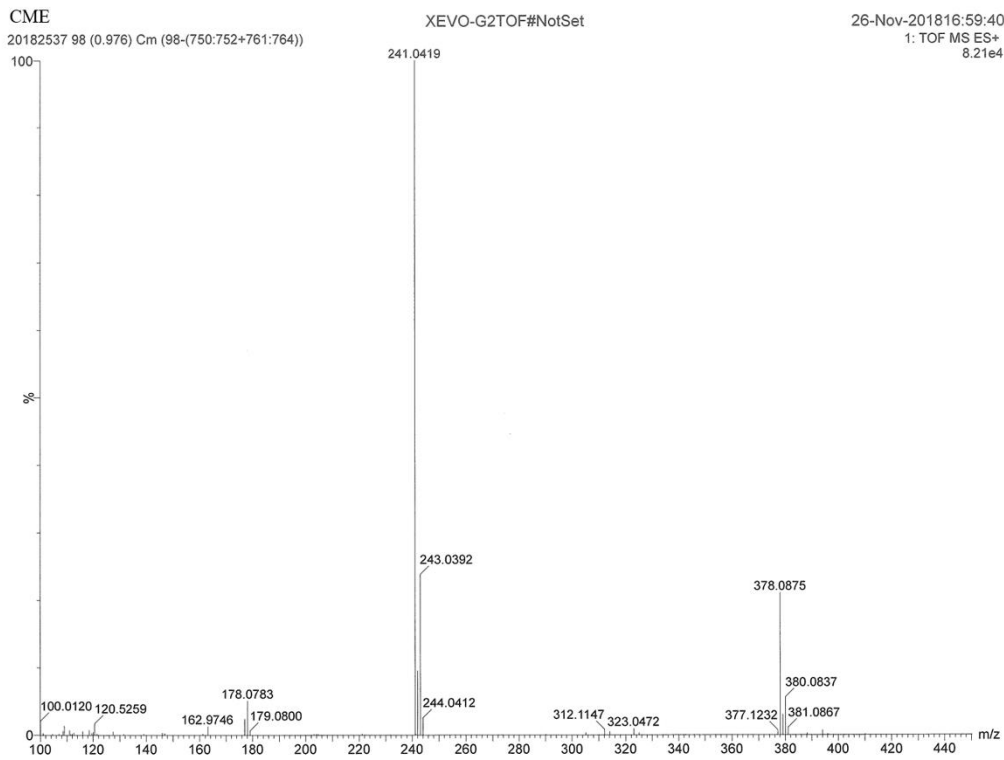


Fig. S34 MS of CME

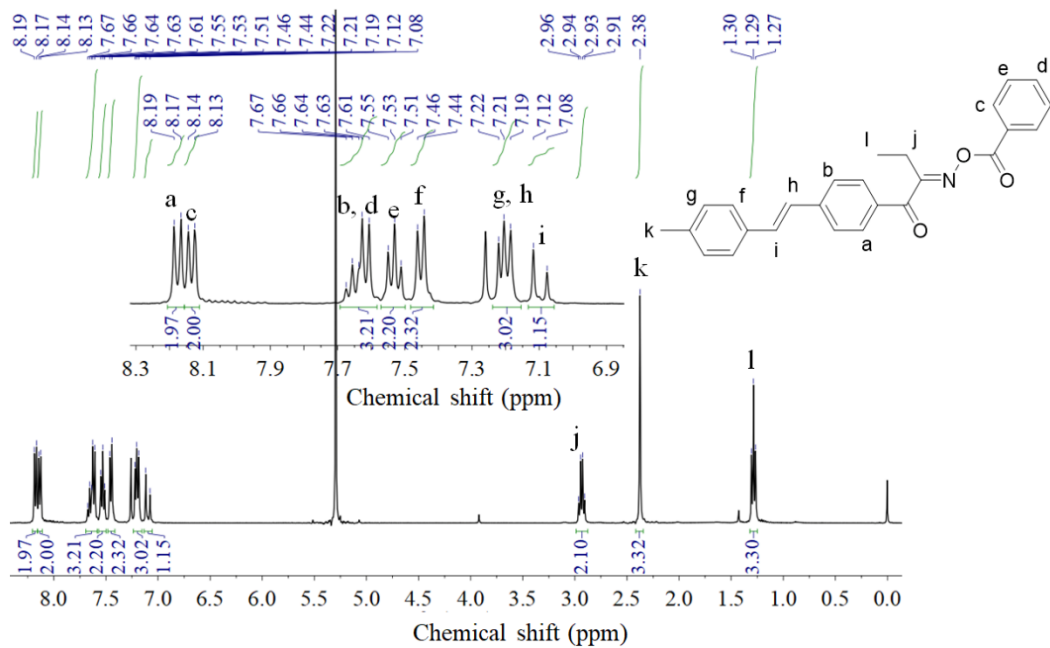


Fig. S35 $^1\text{H-NMR}$ spectrum of MPE in CDCl_3

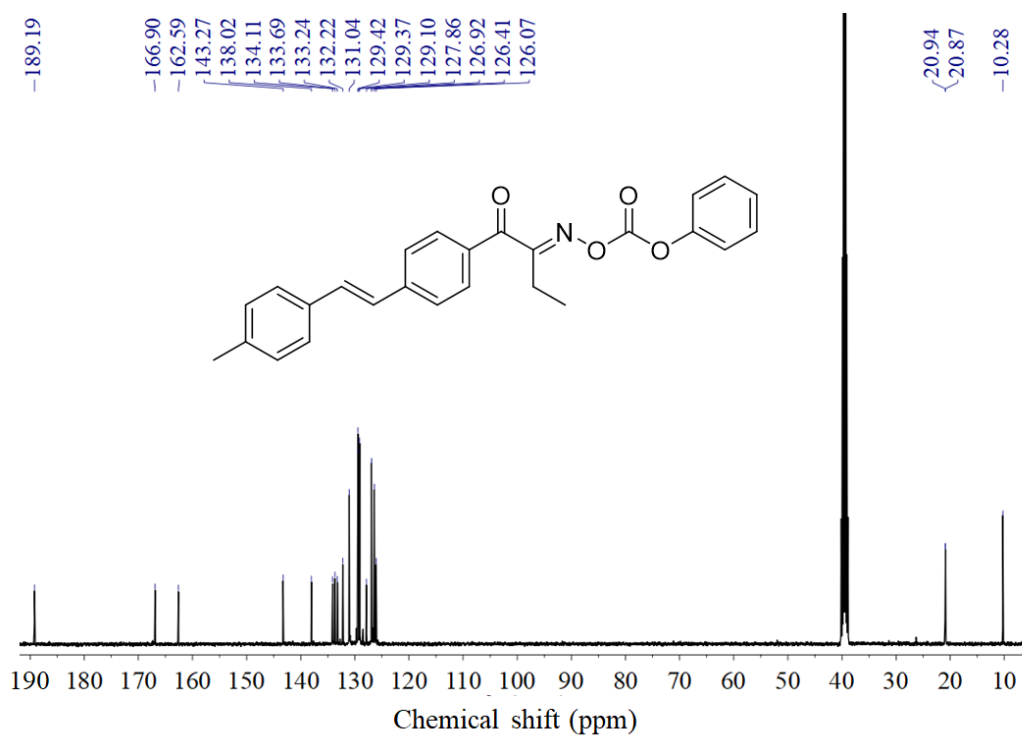


Fig. S36 $^{13}\text{C-NMR}$ spectrum of MPE in CDCl_3

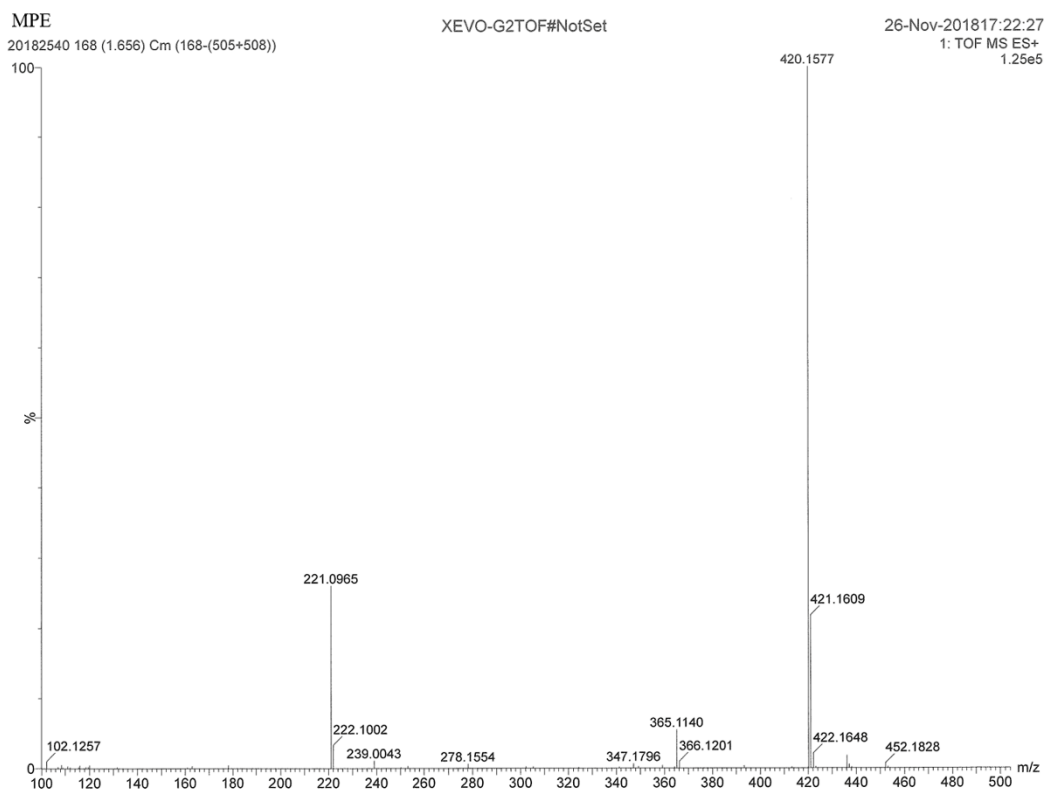


Fig. S37 MS of MPE

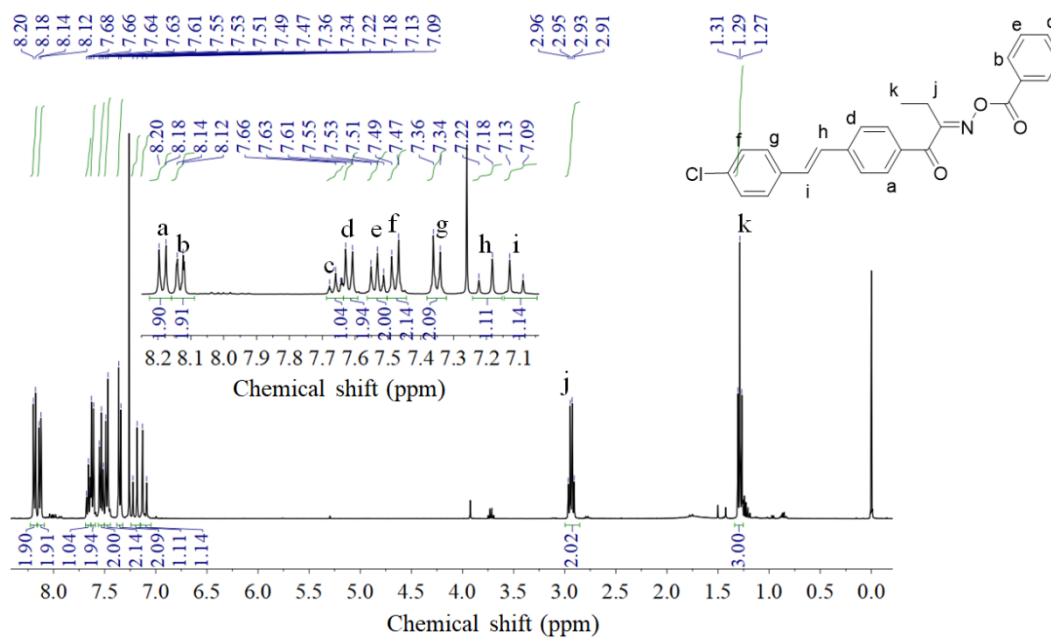


Fig. S38 ¹H-NMR spectrum of CPE in CDCl₃

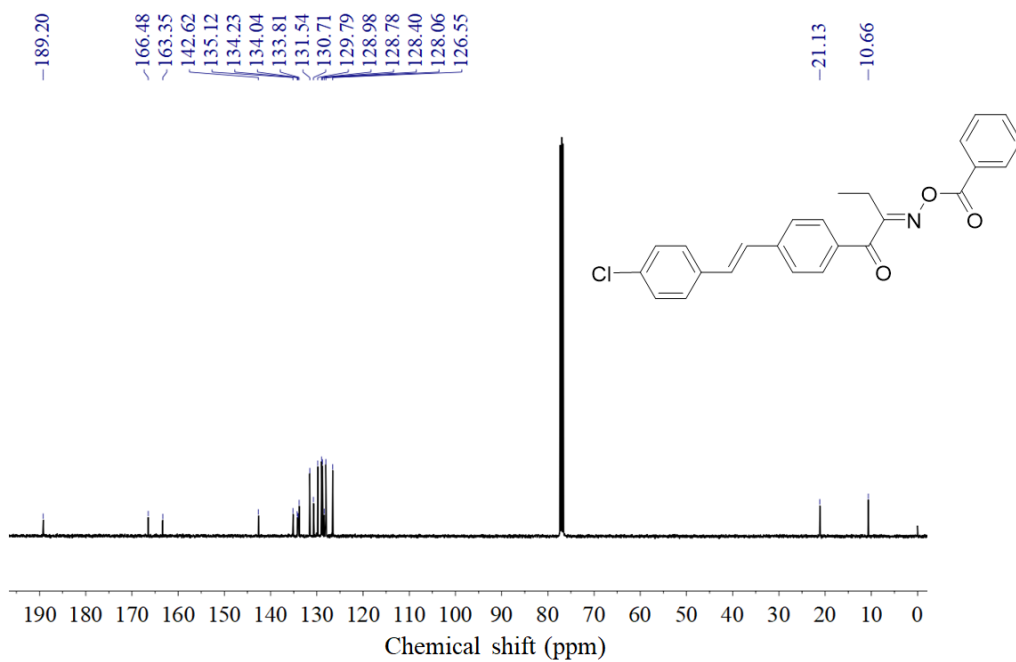


Fig. S39 ^{13}C -NMR spectrum of **CPE** in CDCl_3

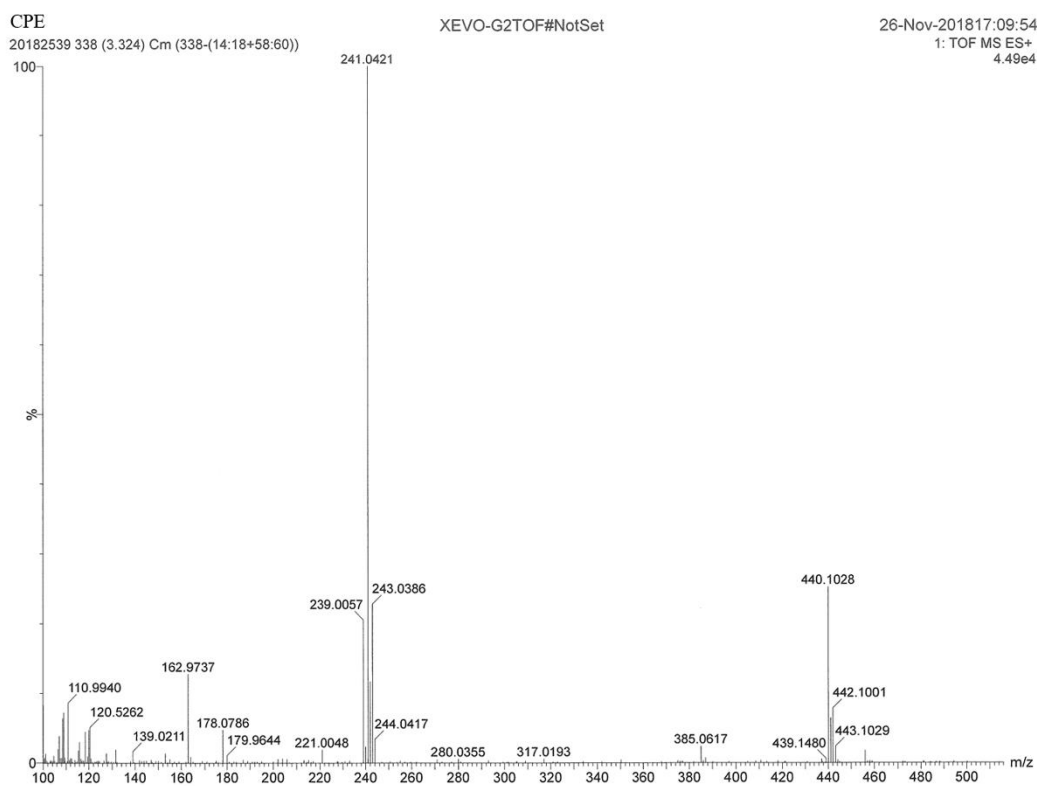


Fig. S40 MS of **CPE**